Journal of Rehabilitation in Civil Engineering 11-3 (2023) 88-106

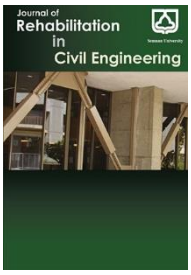

Journal homepage: http://civiljournal.semnan.ac.ir/

An Innovative Approach to Estimate Chloride Diffusion Coefficient in Submerged Concrete Structures Using Soft Computing

Seyed Ali Habibi [1*], Ali Hemmati[2], Hossein Naderpour[3]

1. Ph.D. Student, Department of Civil Engineering, Semnan Branch, Islamic Azad University, Semnan, Iran.
2. Assistant Professor, Department of Civil Engineering, Semnan Branch, Islamic Azad University, Semnan, Iran.
3. Professor, Faculty of Civil Engineering, Semnan University, Semnan, Iran.
Corresponding author: *seidali.habiby@yahoo.com*

ARTICLE INFO

Article history:
Received: 21 August 2022
Revised: 22 October 2022
Accepted: 06 December 2022

Keywords:
Corrosion;
Markov chain;
Support vector machine;
Ensemble learning;
K-Nearest neighbors.

ABSTRACT

Corrosion is one of the most important and common factors in the destruction of structures. Among all kinds of structures, corrosion of submerged structures is of great importance and prevalence due to the impossibility of direct visibility, high reconstruction cost and special environmental conditions. The work done in the field of corrosion of these structures has mainly dealt with modeling the problem in the form of mathematical formulation or using soft computing methods. The work that has established the connection between these two methods has not been done, to the best of our knowledge. This article aims to develop a model in order to estimate the chloride diffusion coefficient in rebar corrosion in submerged concrete structures. Present study seeks to address the estimation of chloride diffusion coefficient, which is one of the determinant factors in computing the corrosion time/rate of rebar's. In this article, using the Monte Carlo sampling method and the formulas available for chloride diffusion coefficient, we produced 2000 artificial data samples. A variety of methods such as support vector machines (e.g., linear, quadratic, cubic, Gaussian), K-nearest neighbors (fine, medium, coarse KNN), and two methods of ensemble learning (bagged tree, subspace discriminant) are applied to predict the chloride diffusion coefficient. The results indicated that the quadratic support vector method (with 93.5% accuracy) is the best technique in estimating the chloride diffusion coefficient. Best KNN model (medium KNN) and best ensemble method (bagged tree) have accuracy of 59.9% and 81.3%, resp.

How to cite this article:
Habibi, S. A., Hemmati, A., & Naderpour, H. (2023). An Innovative Approach to Estimate Chloride Diffusion Coefficient in Submerged Concrete Structures Using Soft Computing. Journal of Rehabilitation in Civil Engineering, 11(3), 88-106.
https://doi.org/10.22075/JRCE.2022.28128.1697

1. Introduction

The process of corrosion and destruction in a structure is generally divided into three stages. The first stage, which occurs in a very long time, is the time of the sample exposure until the chlorine or sulfate is fully dispersed at the surface of the structure. The second stage is the process of chlorine diffusion into the structure, and the exposure time of steel and rebar buried inside the concrete, during which the rebar is affected by destructive factors, resulting in forming corrosion cell in the structure. In the third stage, metal corrosion begins after the cell formation, which causes a destruction and area reduction in structure and rebar, resulting in creating a negative effect on the structural strength. Moreover, it is necessary to strengthen and repair the damaged structure in advance before conducting the third stage. Hence, it is essential to estimate and predict when the metal corrosion may begin. In this regard, detailed inspection and monitoring are required for structural performance and structural behavior. Fig. 1 presents a picture of a deteriorated rebar due to corrosion.

Fig. 1. a picture of a deteriorated rebar due to corrosion.

The corrosion rate depends on many parameters such as the initial diameter of the steel bar, the density and, weight of the steel lining, Faraday constant, steel elbow profile, the bandgap flexibility, Poisson ratio, concrete elastic modulus, creep coefficient, concrete thickness, concrete expansion coefficient, rebar penetration depth, corrosion product density, thickness of corrosion products for production, tensile stress on concrete, corrosion-resistant material, porous bonding thickness around steel/concrete, interface, chlorine concentration at surface, water to cement ratio and exposure time [1].

In this regard, the small number of effective parameters reduces the accuracy of the model and is not practical in some cases. In [2], for example, the corrosion procedure formula, known as the fib model (2006), was modeled for the Persian Gulf environment, and it was found that the formula is not accurate enough to model and estimate corrosion time in the concerned environment as a result of disregarding some parameters which act differently in different environments. Applying artificial intelligence-based methods, combining formulas, applying dissimilar formulas to generate samples, and interpolating the results in some unknown examples would contribute to solving the problem.

It is noteworthy to mention that soft computing methods are powerful tools in finding the relationship between the corrosion rate and the factors affecting it. Atha and Jahanshahi [3] applied deep learning and neural network methods to detect corrosion. Moreover, corrosion flow in steel was investigated in [4] as such; the neural network was applied to find steel corrosion in concretes without cross reinforcement. In [3], artificial neural networks, support vector machines, regression and classification trees, linear regression and collective learning methods [5]

were used in order to compute the corrosion and pitting rates.

Jiménez-Come et al. [6] adopted artificial intelligence-based methods to model steel corrosion behavior applying Classification Trees (CT), Discriminant Analysis (DA), K-Neighbors (K-NN), Back-Propagation Neural Networks (BPNN), and Support Vector Machine (SVM) have been used. Furthermore, the researchers applied the aforementioned tools to inquire about the effect of chloride solutions NaCl and MgCl as well as different environmental conditions such as chlorine ion concentration, temperature, and pH on corrosion behavior.

The Influence of Environmental Factors on Concrete Evaporation Rate is modeled in [7]. In [8], the neural network and fuzzy logic were to estimate the corrosion rate of a solution containing 3.5% by weight of salts. Chen and Zang [9] proposed an artificial immune pattern recognition (AIPR) method to classify the damages to the structure and detect the main parameters controlling chloride diffusion, applying long-range data using ensemble learning methods. To this end, the models were taught to use a dataset consisting of variables that described the composition of concrete mix materials, new and hard properties, field conditions, and chloride profiles. The hardening properties of SCCs, including compressive strength, flexural strength, tensile strength, water absorption, and electrical resistance, were contemplated as well in their study. Taffese and Sistonen [10] provided an artificial neural network (ANN) model to model the concrete corrosion processes in sewage ducts. Recent advances in computing approaches lead to successful employing soft computing and reliability based methods in civil engineering context [11–18].

Researchers in [4] employed resistivity and resistivity measurement methods in accordance with neural networks to evaluate the steel corrosion rate in concrete while disregarding reinforcement. The results revealed that the corrosion density of steel-reinforced concrete could be predicted by applying an artificial neural network based on the parameters determined by two methods measuring non-destructive strength. In [19], some approaches based on a different neural network were suggested to assess corrosion at metal surfaces. In addition, soft computing approaches were successfully implemented by different researchers in the context of civil engineering for shear strength prediction of reinforced concrete shear wall [20], modeling of asphalt mixtures dynamic [21], forecasting sensitivity of treated subgrade soil [22], Durability and Resistance forcasting of Cement [23], moment capacity estimation of ferrocement members [24], etc.

In this paper, we estimated the ion-chloride penetration coefficient applying soft-computation methods. To the best of our knowledge, no study has researched the use of the artificial intelligence-based methods in estimating the chloride ion diffusion coefficient. Furthermore, as a result of the lack of appropriate datasets in this field (existing data are almost less than 100 training examples), an approach based on Markov Chain Monte Carlo (MCMC) sampling is used to generate 2000 data samples using diffusion-related formulas addressed in literature. 200 samples of this generated dataset are represented in Appendix 1. Regarding the objectives of this study, support vector support (SVM), K-nearest neighbors (KNN), and

ensemble learning methods were adopted. In the support vector machine method, four variants of SVM (namely linear, quadratic, cubic and Gaussian kernels) were considered. In the KNN, fine, medium, and coarse KNNs were adopted. Ensemble bagged tree and subspace discriminant was also examined in the ensemble learning method. MATLAB software was applied for modeling in the present study as well. In estimating the chloride diffusion coefficient, the SVM with quadratic order kernel and the accuracy of 93.5% was selected as the best method.

The outline of this article is as follows: In the second section, a brief overview of artificial intelligence-based methods is proposed. The third section describes a base model and the formulas used in the corrosion procedure. Section 4 is devoted for proposed methodology to produce artificial dataset for ANN models. Section 5 evaluates the accuracy of the developed models. Section 6 discusses about profits and limitations of proposed methodology, and the last section will conclude the study.

2. An Overview of Soft Computing-Based Methods

Artificial neural networks (ANNs) are developed based on the mathematical models derived from the activity of neurons in the human neural network, in which a collection of sampled data is provided to train a network of layered neurons. The term 'training' refers to finding missing parameters that make an input have a specified output. The most common type of parameter is the synaptic weights of each neuron, reflecting the degree of significance for each of the input features in begetting the output. These weights act like the coefficients of a decision hyper plane equation, which separates the data from a specific output category from data from the other categories.

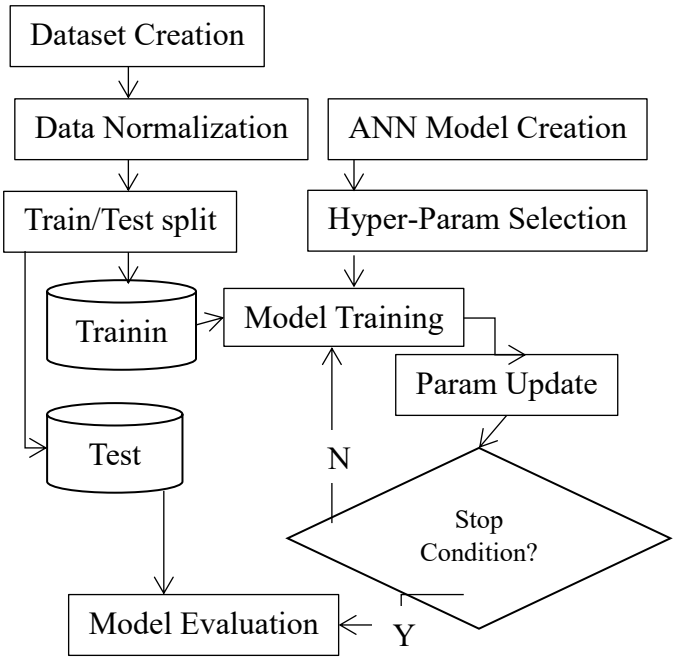

Fig. 2. General scheme of an artificial neural network.

Fig. 2 depicts the general schematic of artificial neural networks. What makes various neural network methods unique is the relationship between neurons, the network training method, manner of determining the values of the interface weights, and the type of mobility function for each neuron. The methods applied in this article are discussed below in brief.

2.1. Support Vector Machine

The supervised neural network methods require input training data and their expected output. Each input sample has several attributes that contain significant features affecting the output. An ANN is to compute the degree of significance of each input in producing an output value. In some neural networks, the concern is to provide a structure for the neural network in such a way that the

estimation error is minimized. In the SVM as a particular kind of neural network, nevertheless, in addition to reducing the estimation error, increasing the margin of the decision page for each of the classes is of the essence [25]. This feature enables the SVM to be better generalized to non-training data. The SVM loss function is defined as (Eq. 1). Fig. 3 depicts how to separate input data applying the SVM decision surface. It also reveals the importance of increasing the margin between the decision surface and the data in different classes.

$$\min \frac{1}{2}||\omega||^2 + C\sum_{i=1}^{n}\zeta_i\,,$$

$$s.t.\, y_i(w^T x_i + b) \geq 1 - \zeta_i,\ \ \zeta_i \geq 0.\, i = 1, \ldots, m. \qquad (1)$$

Where, C is as a regularization term, balancing two criteria of maximum margin (ω) and minimum error (ζ). Moreover, x, w, b are input vector, weight matrix and bayas vector, resp.

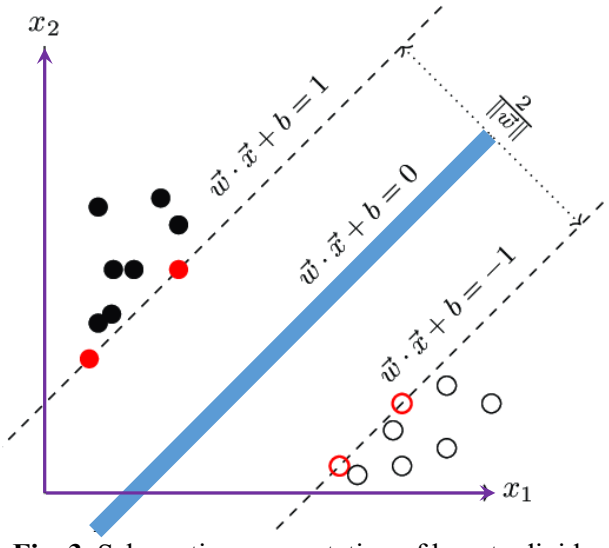

Fig. 3. Schematic representation of how to divide input data into two categories of output using the SVM decision surface.

2.2. K-Nearest Neighbors

KNN is a non-parametric classification method. It is an instance-based learning algorithm in which the function is approximated locally. An input data is assigned to the class or category, which is most common among its *k* nearest neighbors. And if k=1, the input is simply assigned to the class, to which the nearest neighbor belongs. Neighbors and nearest neighbors are computed applying the criterion 1/d, where *d* is a distance criterion.

2.3. Ensemble Learning

In machine learning, ensemble methods consists of a concrete finite set of alternative models to improve the predictive performance of the whole system than what could be obtained from any of the constituent learning algorithms alone. Machine learning ensemble typically allows for some flexible structure to exist among those alternatives.

Different methods for ensemble learning have been proposed in literature. Ensemble bagged tree, and ensemble subspace discriminant are two wellknown ensemble methods. In ensemble bagged tree, firstly some bootstrapped datasets are generated. For each bootstrapped set, the number of elements selected is the same as the original training dataset, but elements are chosen randomly with replacement. Thereafter, each of the bootstrapped datasets is given to an instance of the learning model used by the ensemble (e.g., a decision tree) to be trained on.

Subspace discriminant is another ensemble algorithm that combines the predictions from multiple decision trees trained on different

subsets of columns in the training dataset. Randomly varying the columns used to train each contributing member of the ensemble has the effect of introducing diversity into the ensemble and, in turn, can lift performance over using a single decision tree.

3. Introducing the Corrosion Model

Given the different environmental conditions in different geographical regions and the use of distinct materials in different countries, the introduction and implementation of a uniform global bylaw are not possible; consequently, there have been many studies on the rate and time of corrosion in different countries. In this paper, assuming the full saturation of concrete, chloride emission was contemplated as the main cause of chloride penetration in concrete. In the following, we will review two famous models of corrosion ([26], [27]), which data generation using the combination of these two models in the MCMC framework, has led us to an artificially rich dataset for applying artificial intelligence methods.

The load and resistance factor design (LRFD) of corrosion in chloride-based corrosion is estimated applying the following equation [26], [28]:

$$g(X,t) = C_{th} - C_s\left(1 - erf\frac{x}{2\sqrt{Dt}}\right) \quad (2)$$

If *t* is separated, we have (3):

$$t = \frac{x^2}{4D\left[erf^{-1}\left(1-\frac{C_{th}}{C_s}\right)\right]^2} \quad (3)$$

In Equations (2) and (3), the variable C_{th} represents the threshold chloride concentration, C_s stands for the concentration of surface chloride (in concrete weight percentage), X is the depth of coating (in millimeters), D indicates the chlorine diffusion factor (in millimeter/year), and *t* is the exposure time (in year).

In order to elaborate on the effects of environmental factors (e.g., the actual ambient temperature and test temperature) on the diffusion coefficient, Equations (4) and (5) are used [27]. It is noteworthy to mention, nonetheless, that the emission factors derived from this equation can exclusively be used for ages up to 25 years, and times above 25 years would take uncertain values. This point is deliberated in the next section in terms of producing random samples and applying them in training/testing the ANN data.

$$D = D_{ref} * \left(\frac{t_{ref}}{t}\right)^{\propto} \quad (4)$$

$$D_{ref} = D_{RCM} * exp\left(b_e * \left(\frac{1}{T_{ref}} - \frac{1}{T_{real}}\right)\right) \quad (5)$$

Where the variable t_{ref} represents the age of the concrete in the RCM test (in years), and t is the age of the sample concrete (in years). T_{ref} and T_{real} display the ambient temperature and the actual temperature of the environment (in terms of Kelvin), respectively. Moreover, $b_e$and $\propto$ are two coefficients.

The statistical information for some of the variables *(Cth, Cs, x, Tref , Treal, be, Drcm, Tref, a*) in this study was set in consonance to [29], and the distributions of D is set in accordance with [30] as depicted in Table 1.

In this table, there are more than one mean and a standard deviation for some variables such as C_{th}. In the case of these variables, the test and

training samples are produced uniformly from each of the proposed distributions. Regarding the parameter *t*, given that its values range from 0 to 25, we applied the normal distribution with a mean and standard deviation of 10 and 5. This is due to the positive values below 10 are more likely to be selected than the values ranging from 20 to 25. Furthermore, if the random number generator generates a *t* with a negative value or a value above 25, these values will be reproduced randomly.

Table 1. The statistical information of variables studied according to [29,30].

Coefficient	Mean	STD
C_{th}	0.03 0.07 0.05 0.09	0.009 0.021 0.015 0.027
C_s	0.6 0.8 1 1.2	0.12 0.16 0.2 0.24
X	55 70 85 100	27.5 35 42.5 50
T_{ref}	298	--
T_{real}	307.9125	--
b_e	4800	700
D_{rcm}	37.212	18.606
t_{ref}	0.328	--
a	1.37	0.04
D	35.81 7.1 24.6 43.2	7.162 14.2 41 86.4

4. Implementation and Evaluation

4.1. Proposed Method

In order to apply supervised learning methods, it is requisite to have training data and their target output. Each input sample has several attributes containing the main features affecting the output. In our proposed method, the chloride diffusion coefficient was the expected output. A thorough review of the literature revealed the output characteristics, as described in Section 3. Accordingly, 10 inputs and 1 output characteristics were contemplated for each sample.

Each input data may take different values. In order to produce the training data, we acquired the properties of each input data applying Table 1 that presents the distribution for each of the variables affecting the diffusion coefficient. In this regard, normal distributions were used to generate the data randomly.

Considering the data, the chlorine diffusion coefficient, as an output, was computed by Equation (4). Given that the appropriate distribution of D is illustrated in Table 1 according to [30], D was assumed to be in range from 0 to 400. Hence, the data with a D value above 400 were considered as incompatible data and removed from the training cycle. Moreover, zero-value is inconsistent for D, as it will causes t to be infinite. In practice, there were only a few inconsistent data (0 to 3 out of 2000 samples) in each run of data production procedure.

Since the supervised learning-based methods map the input to one of the limited set of output categories based on the features of the input data, it is requisite to discretize the output data as well. As the data was more dispersed in lower quantities, the categories

were not homogeneously distributed. The breakdown applied for values of D<1 is affiliated to the four categories 0, 0.2, 0.4, and 0.8. For greater values, any data between $(n-1)^2$ and n^2 belonged to the category $(n-1)^2$. In general, a maximum of 2000 samples and 23 output categories were included in the study. To be more precise, 200 samples of the dataset produced by MCMC are presented in Appendix 1.

The data were imported to the SVM, KNN and Ensemble Learning methods for evaluation. In order to evaluate the accuracy of applying these methods, the data should be divided into two train and test data sets. In this paper, the k-fold method (k = 10) was used for this purpose, implying that the data (2000 samples) are divided into k batches. For k times, a batch is dismissed as the test data. After training the neural network with the other nine classes, the test data was reused to evaluate the accuracy of the method. Conclusively, the average precision of the batches was set as the overall accuracy of the method. The general flowchart of the proposed method is illustrated in Fig. 4.

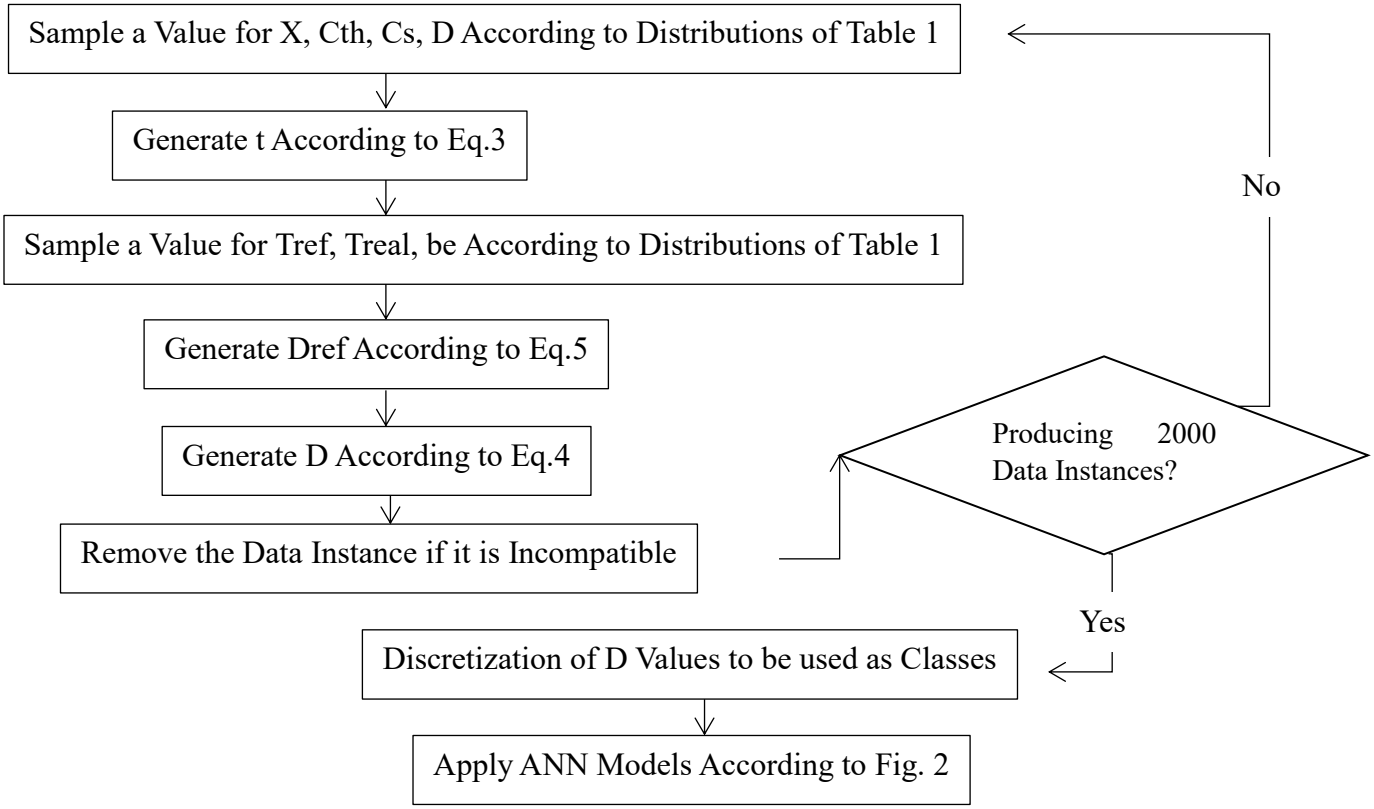

Fig. 4. Flowchart of the Proposed Methodology.

5. Evaluation Results

To evaluate the proposed methodology of using MCMC to relate multiple corrosion formulas and producing artificial dataset, some classifiers are used. The SVM, KNN, and ensemble learning methods were applied to compute the diffusion coefficient based on 11 other variables (t, tref, Tref, Treal, Cth, Cs, a, be, d, Drcm, Dref). We used classification learner application of Matlab R2020 for classifiers. The accuracy of each method is examined below.

5.1 Support Vector Machine

In this section, four versions of the support vector machine (namely linear, quadratic, cubic, and Gaussian kernels) were adopted to estimate the diffusion coefficient of chlorine. In Table 2, the parameters of each SVM method are presented.

Table 2. The Parameters of the SVM Models.

SVM Models	Parameter	Parameter Value
Gucci SVM	Kernel function	Gaussian
	Box constraint level	1
	Kernel scale mode	Manual
	Manual kernel scale	0.83
	Multiclass method	One-vs-one
	Standardize data	yes
Second-class SVM	Kernel function	Quadratic
	Box constraint level	1
	Kernel scale mode	Auto
	Manual kernel scale	1
	Multiclass method	One-vs-one
	Standardize data	yes
Cubic SVM	Kernel function	Cubic
	Box constraint level	1
	Kernel scale mode	Auto
	Manual kernel scale	1
	Multiclass method	One-vs-one
	Standardize data	yes
SVM linear	Kernel function	Liner
	Box constraint level	1
	Kernel scale mode	Auto
	Manual kernel scale	1
	Multiclass method	One-vs-one
	Standardize data	yes

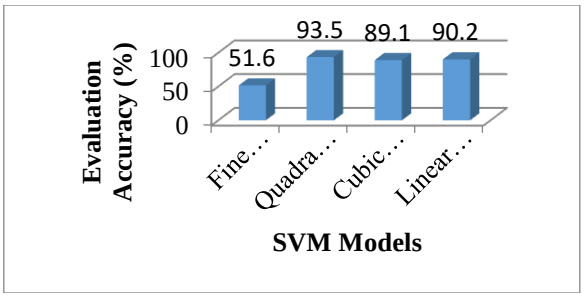

Fig. 5. Accuracy diagram of different versions of the SVM method in predicting chlorine penetration.

Fig. 5 indicates the accuracy of each of the SVM models. As depicted in this figure, SVM with a quadratic kernel function has the best performance for predicting the data. Accuracy of this SVM model is 93.5%. linear and cubic SVM have acceptable performance, as well. However, the performance of Gaussian kernel has been poor. This may be due to the high complexity of this function and the lack of setting of its hyper-parameters.

5.2. K-Nearest Neighbors

In the K-nearest neighbor method, as a data classification method, three different versions were applied for classification: Fine KNN, medium KNN, and coarse KNN. In Table 3, the parameters of each KNN method are portrayed. The accuracy of each of the KNN versions is also illustrated in Fig. 6. Accuracy of all of these models are in range 50-60%. In comparison to SVM models, this may indicate that KNN models are not appropriate for this dataset.

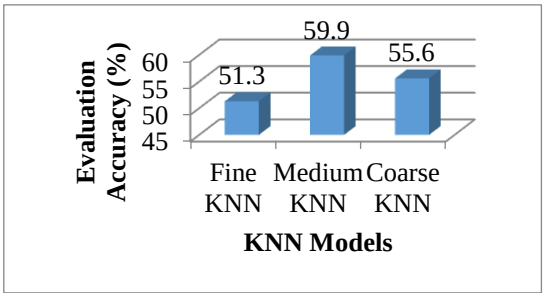

Fig. 6. Accuracy of Different KNN Models in Predicting Chlorine Penetration.

Table 3. Parameters of the KNN Models.

KNN Model	Parameter	Parameter Value
Fine KNN	Number of neighbors	1
	Distance metric	Euclidean
	Distance weight	Equal
	Standardize data	yes
Medium KNN	Number of neighbors	10
	Distance metric	Euclidean
	Distance weight	Equal
	Standardize data	yes
Coarse KNN	Number of neighbors	100
	Distance metric	Euclidean
	Distance weight	Equal
	Standardize data	yes

5.3. Ensemble Learning Method

In this section, two ensemble learning methods (namely ensemble bagged tree and the subspace discriminant) were used. The accuracy of each of these methods is displayed in Table 3. The ensemble learning methods are usually applied as these methods can combine the advantages of several learning methods. If a good method is combined with a few bad or moderate methods, the result is not necessarily more accurate than the best one. Table 4 indicates the parameters of each ensemble learning method. The accuracy of ensemble learning methods in predicting chlorine penetration is shown in Fig. 7. As can be seen in the figure, the accuracy of subspace KNN-based ensemble method is 45.4% which is poor. As seen in the previous section, all KNN classifiers have poor performance in this regard, as well. However, bagged tree ensemble learning (with 81.3% accuracy) has better performance. Of course, the performance of decision tree-based methods has been weaker than SVM-based methods, as well.

Table 4. Parameters of the Used Ensemble Learning Methods.

Ensemble Method	Parameter	Parameter value
Ensemble bagged tree	Ensemble method	Bag
	Learner type	Decision tree
	Maximum number of splits	20
	Number of learners	30
	Learning rate	0.1
	Subspace dimension	1
Ensemble subspace Discriminant	Ensemble method	subspace
	Learner type	Discriminant
	Maximum number of splits	20
	Number of learners	30
	Learning rate	0.1
	Subspace dimension	6

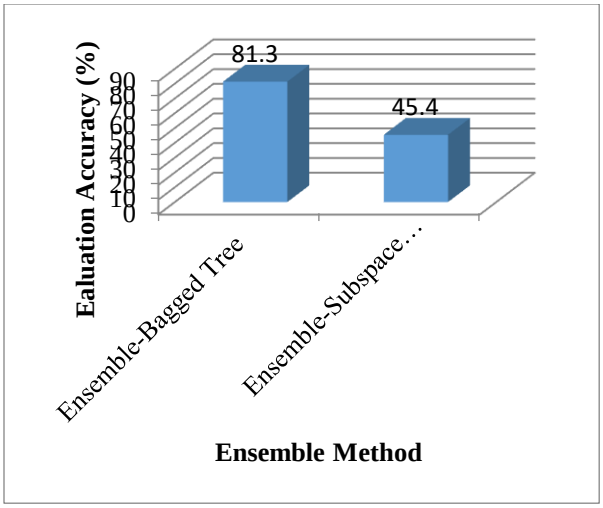

Fig. 7. Accuracy of Ensemble Learning Methods in Predicting Chlorine Penetration.

In the following, for general comparison, the accuracy of the aforementioned methods are graphed (Fig. 8). Fig. 9 displays the computation time required for each of the proposed methods. Generally, SVM models are accurate models with high computation time. KNN models are poor but fast models. Ensemble learning methods are in the middle in terms of speed and accuracy

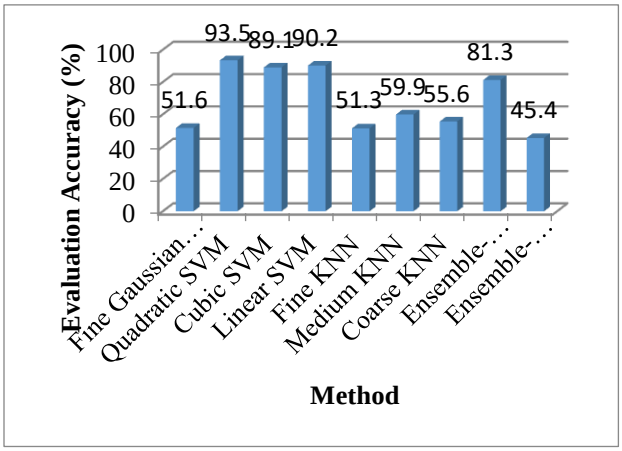

Fig. 8. Accuracy Diagram of Different Methods in Predicting Chlorine Penetration.

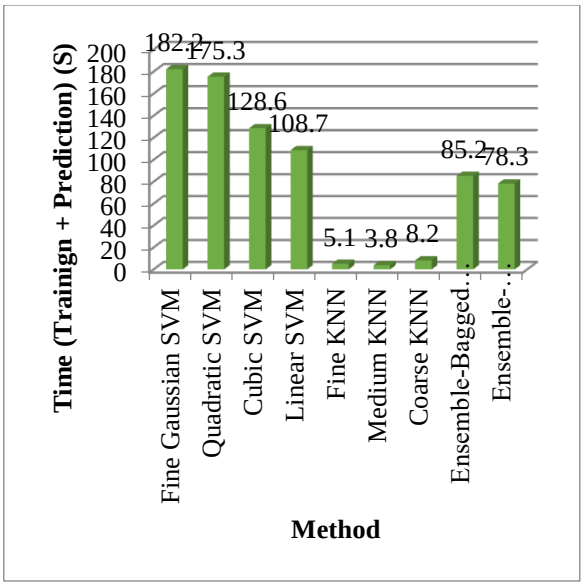

Fig. 9. Computation Time (Training + Prediction) of Different Methods.

The results obtained so far were valid for 10-fold cross validation method utilizing all data. In the following, we separated 75% of the data as train data from the rest of the data and calculated the mean squared error (MSE), mean absolute error (MAE) and accuracy of each method, separately. The results of this comparison is illustrated in Table 5. As can be seen in this table, fine KNN and ensemble-bagged tree methods 100% fitted on the train data, but they have low accuracy on the test data. It can be said that over fitting has happened in these two methods and the model has low generalizability. For Test data, SVM-based methods still have the best accuracy and the lowest amount of errors (MSE and MAE). Among these, quadratic SVM has obtained the best results for test data.

Table 5. Evaluation of methods for 75%/25% split of train/test data.

Model/Criteria	Train			Test		
	MSE	MAE	Acc.	MSE	MAE	Acc.
Fine Gaussian SVM	2.49E+03	11.6203	85.7333	3.16E+03	16.8744	50
Quadratic SVM	673.1722	4.1989	90.2	**648.5966**	**5.264**	**83**
Cubic SVM	313.1837	1.6295	97.3333	854.7752	6.7536	75.4
Linear SVM	1.11E+03	7.652	75.7333	655.5325	6.0624	77
Fine KNN	**0**	**0**	100	898.5326	11.6276	35.2
Medium KNN	1.48E+03	11.9573	52.9333	844.5578	10.3352	48
Coarse KNN	2.43E+03	15.5292	50.1333	2.95E+03	16.4544	50
Ensemble-Bagged Tree	**0**	**0**	**100**	1.44E+03	8.6156	73.4
Ensemble-Subspace KNN	1.98E+03	14.1332	50.4	1.68E+03	12.7764	50.6

6. Discussion

In this paper, it was proposed to benefit from the MCMC approach and corrosion models, to construct artificial dataset. This dataset is utilized to train ANN-based models for corrosion prediction.

Note that the, optimal performance of ANN-based models requires data and the amount of data is very effective on the accuracy of these methods. Considering the high cost of producing real or laboratory data, using the proposed methodology can be effective in reducing the cost of data production. Moreover, by using this method, it is possible to use a large number of corrosion-related formulas, to produce a dataset that considers many factors affecting corrosion.

Of course, along with these advantages, the proposed method also has limitations. Among other methods, the validity of the generated artificial data is lower than the laboratory data. Also, correlation of corrosion formulas may not have been studied and produced data may be weak from this point of view. Of course, in any case, this method can be used in estimating the corrosion time depending on many variables, and also in introducing new models of this subject.

7. Conclusion

Contemplating the significance of the chloride diffusion coefficient in estimating the corrosion rate and corrosion time, the problem with estimating this factor is discussed in this paper. To this end, artificial intelligence methods attributed to the

supervised learning were applied, and the training data samples for each of the effective parameters in the chloride diffusion coefficient were produced using the distributions of parameters proposed in the literature. Consequently, the chlorine diffusion coefficient was computed as the expected output data in supervised learning. The data were used for three types of machine learning methods (namely SVM, KNN and ensemble learning). Among other methods, the accuracy of detecting the correct output category was estimated to be 93.5% for the best version of the SVM (i.e., quadratic SVM). In the KNN, the best accuracy was observed for the medium KNN method with a precision of 59.9%. In the case of ensemble learning methods, the ensemble bagged tree method was 81.3% accurate. In general, it can be concluded that the quadratic SVM has the best accuracy to predict ion chloride diffusion, reflecting the significance of artificial intelligence-based methods in terms of corrosion.

References

[1] Karuppanasamy J, Pillai RG. Statistical Distributions for the Corrosion Rates of Conventional and Prestressing Steel Reinforcement Embedded in Chloride Contaminated Mortar. CORROSION 2017;73:1119–31. https://doi.org/10.5006/2330.

[2] Ramezanianpou AA, Jahangiri E, Moodi F, Ahmadi B. Assessment of the Service Life Design Model Proposed by fib for the Persian Gulf Region. J Oceanogr 2014;5:101–12.

[3] Chou JS, Ngo NT, Chong WK. The use of artificial intelligence combiners for modeling steel pitting risk and corrosion rate. Eng Appl Artif Intell 2017;65:471–83. https://doi.org/10.1016/j.engappai.2016.09.008.

[4] Sadowski L. Non-destructive investigation of corrosion current density in steel reinforced concrete by artificial neural networks. Arch Civ Mech Eng 2013;13:104–11. https://doi.org/10.1016/j.acme.2012.10.007.

[5] Jahangir H, Nikkhah Z, Rezazadeh Eidgahee D, Esfahani MR. Performance Based Review and Fine-Tuning of TRM-Concrete Bond Strength Existing Models. J Soft Comput Civ Eng 2023;7:43–55. https://doi.org/10.22115/scce.2022.349483.1476.

[6] Jiménez-Come MJ, Muñoz E, García R, Matres V, Martín ML, Trujillo F, et al. Pitting corrosion behaviour of austenitic stainless steel using artificial intelligence techniques. J Appl Log 2012;10:291–7. https://doi.org/10.1016/j.jal.2012.07.005.

[7] Papadimitropoulos VC, Tsikas PK, Chassiakos AP. Modeling the Influence of Environmental Factors on Concrete Evaporation Rate. J Soft Comput Civ Eng 2020;4:79–97. https://doi.org/10.22115/scce.2020.246071.1254.

[8] Mousavifard SM, Attar MM, Ghanbari A, Dadgar M. Application of artificial neural network and adaptive neuro-fuzzy inference system to investigate corrosion rate of zirconium-based nano-ceramic layer on galvanized steel in 3.5% NaCl solution. J Alloys Compd 2015;639:315–24. https://doi.org/10.1016/j.jallcom.2015.03.052.

[9] Chen B, Zang C. Artificial immune pattern recognition for structure damage classification. Comput Struct 2009;87:1394–407. https://doi.org/10.1016/j.compstruc.2009.08.012.

[10] Taffese WZ, Sistonen E. Significance of chloride penetration controlling parameters in concrete: Ensemble methods. Constr Build Mater 2017;139:9–23. https://doi.org/10.1016/j.conbuildmat.2017.02.014.

[11] Fakharian P, Rezazadeh Eidgahee D, Akbari M, Jahangir H, Ali Taeb A. Compressive strength prediction of hollow concrete masonry blocks using artificial intelligence algorithms. Structures 2023;47:1790–802. https://doi.org/10.1016/j.istruc.2022.12.007.

[12] Kontoni D-PN, Onyelowe KC, Ebid AM, Jahangir H, Rezazadeh Eidgahee D, Soleymani A, et al. Gene Expression Programming (GEP) Modelling of Sustainable Building Materials including Mineral Admixtures for Novel Solutions. Mining 2022;2:629–53. https://doi.org/10.3390/mining2040034.

[13] Ghanizadeh AR, Ghanizadeh A, Asteris PG, Fakharian P, Armaghani DJ. Developing bearing capacity model for geogrid-reinforced stone columns improved soft clay utilizing MARS-EBS hybrid method. Transp Geotech 2023;38:100906. https://doi.org/10.1016/j.trgeo.2022.100906.

[14] Khademi A, Behfarnia K, Kalman Šipoš T, Miličević I. The Use of Machine Learning Models in Estimating the Compressive Strength of Recycled Brick Aggregate Concrete. Comput Eng Phys Model 2021;4:1–25. https://doi.org/10.22115/cepm.2021.297016.1181.

[15] Rezazadeh Eidgahee D, Haddad A, Naderpour H. Evaluation of shear strength parameters of granulated waste rubber using artificial neural networks and group method of data handling. Sci Iran 2019;26:3233–44. https://doi.org/10.24200/sci.2018.5663.1408.

[16] Naderpour H, Haji M, Mirrashid M. Shear capacity estimation of FRP-reinforced concrete beams using computational intelligence. Structures 2020;28:321–8. https://doi.org/10.1016/j.istruc.2020.08.076.

[17] Naderpour H, Mirrashid M. Proposed soft computing models for moment capacity prediction of reinforced concrete columns. Soft Comput 2020;24:11715–29. https://doi.org/10.1007/s00500-019-04634-8.

[18] Naderpour H, Mirrashid M. Moment capacity estimation of spirally reinforced concrete columns using ANFIS. Complex Intell Syst 2020;6:97–107. https://doi.org/10.1007/s40747-019-00118-2.

[19] Atha DJ, Jahanshahi MR. Evaluation of deep learning approaches based on convolutional neural networks for corrosion detection. Struct Heal Monit 2018;17:1110–28. https://doi.org/10.1177/1475921717737051.

[20] Naderpour H, Sharei M, Fakharian P, Heravi MA. Shear Strength Prediction of Reinforced Concrete Shear Wall

Using ANN, GMDH-NN and GEP. J Soft Comput Civ Eng 2022;6:66–87. https://doi.org/10.22115/SCCE.2022.283486.1308.

[21] Rezazadeh Eidgahee D, Jahangir H, Solatifar N, Fakharian P, Rezaeemanesh M. Data-driven estimation models of asphalt mixtures dynamic modulus using ANN, GP and combinatorial GMDH approaches. Neural Comput Appl 2022;34:17289–314. https://doi.org/10.1007/s00521-022-07382-3.

[22] Onyelowe KC, Rezazadeh Eidgahee D, Jahangir H, Aneke FI, Nwobia LI. Forecasting Shear Parameters, and Sensitivity and Error Analyses of Treated Subgrade Soil. Transp Infrastruct Geotechnol 2022. https://doi.org/10.1007/s40515-022-00225-7.

[23] Salahudeen AB, Jalili M, Eidgahee DR, Onyelowe KC, Kabiri MK. Prediction of Durability, Resilient Modulus and Resistance Value of Cement Kiln Dust-Stabilized Expansive Clay for Flexible Pavement Application Using Artificial Neural Networks. vol. 164. Cham: Springer International Publishing; 2022. https://doi.org/10.1007/978-3-030-77230-7.

[24] Naderpour H, Rezazadeh Eidgahee D, Fakharian P, Rafiean AH, Kalantari SM. A new proposed approach for moment capacity estimation of ferrocement members using Group Method of Data Handling. Eng Sci Technol an Int J 2020;23:382–91. https://doi.org/10.1016/j.jestch.2019.05.013.

[25] Naderpour H, Noormohammadi E, Fakharian P. Prediction of Punching Shear Capacity of RC Slabs using Support Vector Machine. Concr Res 2017;10:95–107. https://doi.org/10.22124/jcr.2017.2417.

[26] Angst UM. Predicting the time to corrosion initiation in reinforced concrete structures exposed to chlorides. Cem Concr Res 2019;115:559–67. https://doi.org/10.1016/j.cemconres.2018.08.007.

[27] Khan MU, Ahmad S, Al-Gahtani HJ. Chloride-Induced Corrosion of Steel in Concrete: An Overview on Chloride Diffusion and Prediction of Corrosion Initiation Time. Int J Corros 2017;2017:1–9. https://doi.org/10.1155/2017/5819202.

[28] Femenias Y, Angst U, Moro F, Elsener B. Development of a Novel Methodology to Assess the Corrosion Threshold in Concrete Based on Simultaneous Monitoring of pH and Free Chloride Concentration. Sensors 2018;18:3101. https://doi.org/10.3390/s18093101.

[29] Ghanooni Bagha M, Asgarani S. Influence of effective chloride corrosion parameters variations on corrosion initiation. Modares Civ Eng J 2017;17.

[30] Nogueira CG, Leonel ED. Probabilistic models applied to safety assessment of reinforced concrete structures subjected to chloride ingress. Eng Fail Anal 2013;31:76–89. https://doi.org/10.1016/j.engfailanal.2013.01.023.

Appendix 1. 200 instances of data samples generated by MCMC and used to train the ML models.

	D	t	C_s	C_{th}	d	T_{ref}	T_{real}	t_{ref}	a	b_e	D_{rcm}
1	1.682	3.24	0.562	0.024	20.283	298	307.913	0.328	1.442	5221.82	31.409
2	0.247	10.24	0.443	0.026	11.932	298	307.913	0.328	1.416	4257.65	21.246
3	0.518	14.44	0.405	0.025	58.812	298	307.913	0.328	1.401	4406.87	67.579
4	0.391	11.56	0.474	0.022	37.527	298	307.913	0.328	1.361	3925.93	32.709
5	0.321	10.24	0.444	0.018	33.624	298	307.913	0.328	1.367	3481.02	26.796
6	0.446	11.56	0.515	0.03	18.964	298	307.913	0.328	1.389	3844.99	41.529
7	0.165	21.16	0.438	0.028	68.993	298	307.913	0.328	1.389	4768.27	34.678
8	0.76	4	0.575	0.044	15.622	298	307.913	0.328	1.464	4688.94	23.017
9	0.647	12.96	0.549	0.024	50.068	298	307.913	0.328	1.34	4749.04	57.106
10	0.85	7.84	0.547	0.023	15.167	298	307.913	0.328	1.358	5088.52	41.699
11	0.585	11.56	0.652	0.032	51.611	298	307.913	0.328	1.401	4557.8	54.826
12	0.517	4.84	0.58	0.038	29.268	298	307.913	0.328	1.391	4228.28	15.152
13	0.667	10.24	0.568	0.042	88.929	298	307.913	0.328	1.328	4899.7	40.594
14	0.81	11.56	0.368	0.025	51.4	298	307.913	0.328	1.346	5871.55	56.426
15	0.947	4.84	0.594	0.027	80.076	298	307.913	0.328	1.375	5191.45	27.756
16	1.129	7.84	0.864	0.033	31.303	298	307.913	0.328	1.418	5862.83	64.359
17	0.163	17.64	0.663	0.03	75.839	298	307.913	0.328	1.379	4417.44	26.602
18	0.109	17.64	0.684	0.025	59.382	298	307.913	0.328	1.46	4144.44	23.802
19	0.754	5.76	0.437	0.036	0.562	298	307.913	0.328	1.358	5261.48	25.994
20	0.466	9	0.637	0.031	45.787	298	307.913	0.328	1.375	4523.04	28.415
21	0.327	14.44	0.511	0.037	56.381	298	307.913	0.328	1.355	4602.43	37.386
22	0.529	9	0.657	0.028	25.3	298	307.913	0.328	1.351	4333.48	30.04
23	10.115	1.96	0.424	0.037	72.524	298	307.913	0.328	1.4	4478.92	87.395
24	0.309	11.56	0.745	0.036	50.65	298	307.913	0.328	1.373	5472.23	23.172
25	0.68	10.24	0.452	0.028	97.294	298	307.913	0.328	1.327	5142.3	43.743
26	0.492	12.96	0.531	0.018	27.669	298	307.913	0.328	1.408	5002.32	51.325
27	0.774	4.84	0.77	0.034	48.495	298	307.913	0.328	1.356	5516.17	16.564
28	0.297	6.76	0.674	0.029	40.318	298	307.913	0.328	1.323	4305.31	11.095
29	0.779	9	0.46	0.041	44.858	298	307.913	0.328	1.398	5683.15	47.15
30	0.466	11.56	0.792	0.028	33.079	298	307.913	0.328	1.311	5262.77	29.143
31	5.309	1.96	0.487	0.033	43.649	298	307.913	0.328	1.324	4388.27	46.814
32	0.715	12.96	0.668	0.029	57.504	298	307.913	0.328	1.367	5558.1	66.376
33	0.36	10.24	0.666	0.025	12.401	298	307.913	0.328	1.344	3955.3	25.599
34	0.267	16	0.885	0.03	57.745	298	307.913	0.328	1.391	5151.4	37.884
35	1.204	3.24	0.733	0.034	73.276	298	307.913	0.328	1.272	4471.6	17.715
36	0.557	9	0.594	0.028	64.163	298	307.913	0.328	1.376	5112.53	32.292
37	1.66	5.76	0.564	0.025	55.307	298	307.913	0.328	1.34	5002.83	46.458
38	0.59	4.84	0.254	0.036	65.808	298	307.913	0.328	1.469	4533.97	19.196
39	0.396	7.84	0.719	0.022	71.361	298	307.913	0.328	1.397	5514.19	19.043
40	0.334	17.64	0.413	0.018	43.278	298	307.913	0.328	1.337	5330.89	39.01
41	1.449	4.84	0.562	0.031	60.247	298	307.913	0.328	1.354	4408.54	34.491
42	0.323	23.04	0.712	0.02	87.169	298	307.913	0.328	1.363	5671.4	59.838
43	0.164	4	0.643	0.016	17.549	298	307.913	0.328	1.438	3827.95	5.17
44	0.783	11.56	0.632	0.031	81.55	298	307.913	0.328	1.346	5710.05	52.168
45	12.363	1	0.53	0.035	65.846	298	307.913	0.328	1.397	5367.89	53.693
46	3.013	2.56	0.511	0.025	81.123	298	307.913	0.328	1.372	5785.43	36.784
47	0.462	10.24	0.575	0.034	69.001	298	307.913	0.328	1.375	4672.97	35.196
48	1.46	5.76	0.702	0.018	65.559	298	307.913	0.328	1.334	4864.17	39.479
49	0.191	16	0.52	0.03	38.536	298	307.913	0.328	1.371	4478.39	27.384

50	1.12	6.76	0.618	0.02	48.582	298	307.913	0.328	1.371	5029.79	42.234
51	0.579	14.44	0.551	0.022	37.852	298	307.913	0.328	1.404	3946.73	78.415
52	0.686	6.76	0.499	0.022	38.22	298	307.913	0.328	1.431	3729.13	36.629
53	0.478	11.56	0.486	0.009	46.769	298	307.913	0.328	1.421	4862.91	44.876
54	0.241	14.44	0.601	0.037	56.188	298	307.913	0.328	1.387	4644.76	31.209
55	0.541	11.56	0.654	0.014	24.744	298	307.913	0.328	1.391	4663.6	49.89
56	1.43	9	0.418	0.03	58.989	298	307.913	0.328	1.362	4703.49	82.442
57	1.04	7.84	0.511	0.033	44.645	298	307.913	0.328	1.365	5464.3	52.207
58	0.119	14.44	0.675	0.022	44.977	298	307.913	0.328	1.369	4119.58	14.811
59	4.471	1.96	0.517	0.03	44.683	298	307.913	0.328	1.365	4959.69	39.66
60	0.396	9	0.658	0.049	45.718	298	307.913	0.328	1.384	4589.86	23.921
61	0.238	14.44	0.699	0.039	86.365	298	307.913	0.328	1.399	4532.65	30.954
62	2.173	5.76	0.476	0.026	44.735	298	307.913	0.328	1.39	4941.38	70.104
63	0.161	10.24	0.679	0.023	77.565	298	307.913	0.328	1.418	4651.01	13.919
64	1.03	7.84	0.585	0.027	55.615	298	307.913	0.328	1.388	3678.99	65.611
65	0.611	11.56	0.642	0.021	18.475	298	307.913	0.328	1.325	5062.96	44.399
66	2.27	2.56	0.469	0.035	41.397	298	307.913	0.328	1.37	4619.24	29.793
67	0.42	12.96	0.637	0.027	54.224	298	307.913	0.328	1.355	4140.46	44.047
68	9.688	1.44	0.538	0.008	66.982	298	307.913	0.328	1.418	4749.23	57.128
69	0.412	12.96	0.633	0.042	46.382	298	307.913	0.328	1.406	3945.18	52.741
70	0.571	10.24	0.506	0.032	62.767	298	307.913	0.328	1.299	4500.73	30.971
71	0.671	10.24	0.424	0.038	82.173	298	307.913	0.328	1.334	4961.24	43.841
72	5.35	1.96	0.569	0.028	32.099	298	307.913	0.328	1.327	4553.34	44.842
73	0.237	11.56	0.505	0.025	27.159	298	307.913	0.328	1.377	4232.65	20.367
74	0.286	9	0.641	0.025	39.897	298	307.913	0.328	1.379	4841.06	18.568
75	0.998	7.84	0.544	0.008	57.857	298	307.913	0.328	1.401	4527.25	63.283
76	1.702	3.24	0.705	0.035	63.577	298	307.913	0.328	1.418	5172.24	26.628
77	0.136	17.64	0.626	0.052	23.137	298	307.913	0.328	1.374	4393.99	21.347
78	0.3	14.44	0.545	0.031	40.608	298	307.913	0.328	1.384	4677.37	38.018
79	0.327	14.44	0.619	0.035	62.21	298	307.913	0.328	1.308	4677.62	29.622
80	0.447	14.44	0.635	0.041	69.835	298	307.913	0.328	1.349	4379.59	47.769
81	15.71	1	0.688	0.033	80.063	298	307.913	0.328	1.366	4851.49	59.446
82	2.304	4.84	0.601	0.04	18.111	298	307.913	0.328	1.399	3338.21	81.509
83	0.222	14.44	0.237	0.042	52.966	298	307.913	0.328	1.4	5003.31	29.072
84	0.278	19.36	0.694	0.02	12.102	298	307.913	0.328	1.348	5740.44	39.353
85	0.719	11.56	0.696	0.035	52.782	298	307.913	0.328	1.3	5369.4	43.261
86	1.289	9	0.629	0.04	60.188	298	307.913	0.328	1.356	5609.11	72.233
87	0.249	12.96	0.528	0.03	94.443	298	307.913	0.328	1.367	4699.23	25.412
88	0.465	5.76	0.563	0.033	46.694	298	307.913	0.328	1.344	3629.25	18.307
89	0.617	7.84	0.552	0.038	78.557	298	307.913	0.328	1.388	4754.48	32.876
90	3.104	3.24	0.654	0.04	30.697	298	307.913	0.328	1.359	5356.08	43.793
91	0.683	10.24	0.562	0.031	13.982	298	307.913	0.328	1.336	4299.12	45.916
92	0.444	7.84	0.497	0.035	91.991	298	307.913	0.328	1.396	3700.96	28.718
93	0.46	14.44	0.577	0.015	70.159	298	307.913	0.328	1.357	4960.11	51.974
94	0.122	16	0.51	0.035	81.594	298	307.913	0.328	1.467	3788.99	26.321
95	0.433	5.76	0.568	0.016	63.368	298	307.913	0.328	1.437	4349.26	19.553
96	0.705	4.84	0.416	0.033	14.149	298	307.913	0.328	1.339	3967.6	20.255
97	0.595	10.24	0.618	0.03	73.056	298	307.913	0.328	1.397	5395	41.489
98	0.276	10.24	0.515	0.025	55.427	298	307.913	0.328	1.382	4355.29	22.183
99	0.937	4.84	0.823	0.033	61.619	298	307.913	0.328	1.323	5016.08	22.384
100	0.777	5.76	0.743	0.038	58.024	298	307.913	0.328	1.379	3501.5	34.397

101	0.179	10.24	0.668	0.032	23.126	298	307.913	0.328	1.365	4462.11	12.713
102	0.377	9	0.502	0.025	77.158	298	307.913	0.328	1.369	4449.89	23.122
103	0.403	10.24	0.562	0.019	36.871	298	307.913	0.328	1.353	3704.34	31.717
104	1.062	11.56	0.537	0.033	51.606	298	307.913	0.328	1.4	5063.99	92.697
105	0.782	9	0.721	0.019	23.18	298	307.913	0.328	1.378	5633.11	45.457
106	0.887	6.76	0.773	0.022	33.76	298	307.913	0.328	1.358	5650.35	34.398
107	0.435	7.84	0.68	0.03	12.704	298	307.913	0.328	1.35	5060.87	18.565
108	0.897	9	0.704	0.013	66.855	298	307.913	0.328	1.413	5826.25	58.43
109	0.506	9	0.813	0.029	46.555	298	307.913	0.328	1.383	4116.31	33.008
110	0.303	11.56	0.63	0.013	66.594	298	307.913	0.328	1.353	3587.33	26.097
111	0.197	11.56	0.476	0.046	24.456	298	307.913	0.328	1.487	4750.28	27.617
112	0.556	7.84	0.559	0.031	40.354	298	307.913	0.328	1.468	4503.25	38.605
113	1.179	7.84	0.619	0.032	29.012	298	307.913	0.328	1.403	5042.04	60.591
114	9.704	1.96	0.371	0.031	37.655	298	307.913	0.328	1.367	5576.55	69.425
115	0.822	10.24	0.579	0.043	53.613	298	307.913	0.328	1.291	5095.57	45.597
116	3.676	4	0.67	0.03	58.89	298	307.913	0.328	1.438	5355.15	77.527
117	0.351	5.76	0.598	0.041	60.151	298	307.913	0.328	1.368	4882.59	12.605
118	0.461	7.84	0.572	0.038	96.321	298	307.913	0.328	1.383	5237.08	25.147
119	3.351	4	0.564	0.012	86.26	298	307.913	0.328	1.323	4840.36	57.661
120	0.455	14.44	0.74	0.029	55.643	298	307.913	0.328	1.401	5737.43	53.052
121	0.612	10.24	0.663	0.024	55.233	298	307.913	0.328	1.396	4883.45	45.682
122	0.276	12.96	0.579	0.045	62.943	298	307.913	0.328	1.369	4757.66	25.363
123	0.564	10.24	0.5	0.018	59.685	298	307.913	0.328	1.402	5326.79	41.089
124	0.658	11.56	0.914	0.034	82.241	298	307.913	0.328	1.351	5377.45	45.471
125	1.442	7.84	0.49	0.026	92.754	298	307.913	0.328	1.373	4909	71.691
126	1.873	6.76	0.667	0.022	64.6	298	307.913	0.328	1.37	5739.24	75.761
127	0.157	17.64	0.63	0.032	71.699	298	307.913	0.328	1.443	4711.37	29.747
128	0.236	16	0.566	0.017	49.129	298	307.913	0.328	1.386	4316.65	32.45
129	0.376	11.56	0.659	0.023	43.572	298	307.913	0.328	1.406	4218.37	38.765
130	0.571	9	0.416	0.044	58.077	298	307.913	0.328	1.426	5181.35	37.55
131	2.024	5.76	0.585	0.025	0.888	298	307.913	0.328	1.319	5143.01	52.234
132	1.719	1.44	0.552	0.026	42.577	298	307.913	0.328	1.413	4081.43	13.231
133	0.222	16	0.638	0.025	42.183	298	307.913	0.328	1.387	5231.27	28.041
134	0.295	9	0.739	0.042	85.052	298	307.913	0.328	1.4	5747.22	17.169
135	0.507	12.96	0.722	0.049	18.739	298	307.913	0.328	1.346	5686.23	43.51
136	0.186	16	0.527	0.02	43.103	298	307.913	0.328	1.406	4543.1	30.202
137	3.171	2.56	0.726	0.025	50.883	298	307.913	0.328	1.419	4148.54	40.685
138	0.795	5.76	0.427	0.051	24.87	298	307.913	0.328	1.381	3995.78	29.424
139	1.072	7.84	0.552	0.027	56.145	298	307.913	0.328	1.406	5393.55	58.727
140	1.304	5.76	0.637	0.014	60.416	298	307.913	0.328	1.332	4734.66	41.856
141	2.366	3.24	0.403	0.033	37.92	298	307.913	0.328	1.392	4756.14	45.614
142	0.045	10.24	0.364	0.022	45.674	298	307.913	0.328	1.393	4191	3.501
143	1.169	6.76	0.374	0.011	67.955	298	307.913	0.328	1.279	5088.93	37.087
144	0.575	6.76	0.434	0.031	73.919	298	307.913	0.328	1.46	4828.45	28.798
145	0.555	9	0.542	0.035	57.262	298	307.913	0.328	1.41	5034.22	40.46
146	0.225	10.24	0.806	0.021	44.495	298	307.913	0.328	1.366	4759.55	17.136
147	0.145	4.84	0.618	0.014	78.83	298	307.913	0.328	1.38	4594.17	4.357
148	0.813	9	0.502	0.011	49.066	298	307.913	0.328	1.345	5575.59	39.873
149	1.024	4.84	0.673	0.042	57.283	298	307.913	0.328	1.401	4666.19	32.364
150	0.932	7.84	0.636	0.036	72.931	298	307.913	0.328	1.338	4882.49	44.882
151	0.949	11.56	0.738	0.039	70.884	298	307.913	0.328	1.347	4258.94	77.413

152	0.567	9	0.501	0.02	74.905	298	307.913	0.328	1.356	5672.23	29.05
153	0.888	6.76	0.469	0.037	47.588	298	307.913	0.328	1.292	5302.59	27.974
154	11.366	1	0.691	0.02	1.966	298	307.913	0.328	1.379	4063.74	51.805
155	0.865	10.24	0.281	0.021	53.261	298	307.913	0.328	1.334	4832.61	51.254
156	1.137	6.76	0.617	0.027	51.367	298	307.913	0.328	1.33	3707.1	51.504
157	0.446	10.24	0.432	0.029	53.738	298	307.913	0.328	1.389	4591.73	35.714
158	0.289	14.44	0.41	0.02	26.724	298	307.913	0.328	1.407	4310.96	38.632
159	1.015	10.24	0.743	0.034	47.082	298	307.913	0.328	1.416	4378.6	95.765
160	0.724	4.84	0.714	0.03	68.876	298	307.913	0.328	1.347	3604.31	18.749
161	0.438	4.84	0.476	0.03	81.612	298	307.913	0.328	1.427	4457.45	14.636
162	0.769	10.24	0.414	0.046	12.439	298	307.913	0.328	1.361	4212.41	58.646
163	0.818	5.76	0.408	0.017	51.507	298	307.913	0.328	1.379	3961.7	30.24
164	0.671	10.24	0.666	0.036	17.46	298	307.913	0.328	1.317	5425.37	34.834
165	1.125	4.84	0.378	0.031	88.891	298	307.913	0.328	1.466	4079.16	41.07
166	0.272	11.56	0.43	0.023	91.208	298	307.913	0.328	1.468	4398.86	34.88
167	0.684	6.76	0.641	0.022	81.318	298	307.913	0.328	1.341	4496.46	28.345
168	0.167	6.76	0.587	0.014	51.77	298	307.913	0.328	1.402	4858.8	8.049
169	0.103	10.24	0.681	0.02	38.937	298	307.913	0.328	1.272	4949.71	5.206
170	0.368	7.84	0.507	0.011	54.857	298	307.913	0.328	1.378	4420.45	18.147
171	0.239	10.24	0.615	0.027	68.62	298	307.913	0.328	1.408	4369.82	19.851
172	0.654	9	0.589	0.033	71.023	298	307.913	0.328	1.373	5331	37.313
173	0.389	10.24	0.809	0.033	44.069	298	307.913	0.328	1.368	4354.93	30.419
174	0.218	19.36	0.547	0.024	7.502	298	307.913	0.328	1.331	4910.36	31.303
175	23.107	1	0.497	0.028	72.263	298	307.913	0.328	1.35	5117.13	61.239
176	2.274	6.76	0.619	0.027	53.032	298	307.913	0.328	1.349	5485.51	75.797
177	0.334	17.64	0.591	0.039	18.7	298	307.913	0.328	1.377	5358.33	50.974
178	0.38	12.96	0.454	0.028	37.385	298	307.913	0.328	1.486	5143.82	55.103
179	0.62	14.44	0.577	0.028	64.75	298	307.913	0.328	1.324	5437.76	55.209
180	0.488	11.56	0.601	0.032	22.144	298	307.913	0.328	1.293	5174.52	28.927
181	0.114	12.96	0.765	0.033	33.164	298	307.913	0.328	1.401	5387.81	12.033
182	0.912	7.84	0.448	0.019	59.818	298	307.913	0.328	1.365	5167.82	43.458
183	0.319	14.44	0.451	0.013	60.622	298	307.913	0.328	1.434	4828.73	44.682
184	7.813	1.44	0.355	0.03	36.111	298	307.913	0.328	1.396	4978.57	42.736
185	0.097	11.56	0.711	0.039	51.021	298	307.913	0.328	1.331	4102.14	7.547
186	0.61	14.44	0.679	0.024	72.044	298	307.913	0.328	1.315	5090.84	56.055
187	0.331	11.56	0.427	0.032	17.875	298	307.913	0.328	1.399	4282.36	35.101
188	0.229	10.24	0.481	0.017	60.451	298	307.913	0.328	1.409	5271.47	18.931
189	0.534	12.96	0.529	0.01	60.194	298	307.913	0.328	1.344	4703.69	51.822
190	0.26	9	0.518	0.031	38.366	298	307.913	0.328	1.39	5302.92	16.384
191	0.8	7.84	0.654	0.037	44.854	298	307.913	0.328	1.406	5172.5	43.065
192	0.473	14.44	0.613	0.024	46.998	298	307.913	0.328	1.335	5362.27	45.699
193	0.085	21.16	0.61	0.028	47.403	298	307.913	0.328	1.356	5336.6	14.644
194	0.476	7.84	0.718	0.026	38.436	298	307.913	0.328	1.4	4937.52	25.905
195	0.137	14.44	0.458	0.033	67.73	298	307.913	0.328	1.387	3359.9	19.974
196	1.441	6.76	0.662	0.033	73.726	298	307.913	0.328	1.335	5230.95	50.446
197	0.91	10.24	0.828	0.021	32.545	298	307.913	0.328	1.395	5285.49	65.546
198	0.275	14.44	0.651	0.055	73.029	298	307.913	0.328	1.408	5026.99	35.866
199	0.258	14.44	0.71	0.028	11.57	298	307.913	0.328	1.402	3579.64	36.753
200	0.733	9	0.728	0.025	48.377	298	307.913	0.328	1.317	4608.03	37.829